

文章编号: 0258-7106 (2019) 01-0048-13

Doi: 10.1611/j.0258-7106.2019.01.004

# 西藏纳如松多铅锌矿床石英闪长岩成因: 地球化学 及 Sr-Nd-Pb 同位素证据<sup>\*</sup>

龚雪婧<sup>1</sup>, 杨竹森<sup>2\*\*</sup>, 庄亮亮<sup>3</sup>, 马 旺<sup>4</sup>

(1 中国地质科学院地球深部探测中心, 北京 100037; 2 自然资源部成矿规律与资源评价重点实验室 中国地质科学院矿产资源研究所, 北京 100037; 3 中国地质大学地球科学与资源学院, 北京 100083; 4 中国地质科学院地质研究所, 北京 100037)

**摘要** 纳如松多矿区石英闪长岩具有低  $\text{SiO}_2$ 、富  $\text{MgO}$ 、 $\text{CaO}$  的特征, 含 10%~15% 的角闪石, 为准铝质、分异程度较低的高钾钙碱性-钾玄岩系列 I 型花岗岩。岩体发育较弱的 Eu 负异常, 富集强不相容元素 Rb、Th、U, 而亏损 Nb、Ta、Ti 等高场强元素。同位素测试结果显示, 纳如松多石英闪长岩具有相对较高的  $^{87}\text{Sr}/^{86}\text{Sr}$  初始比值(0.709 13~0.709 68)与负的  $\varepsilon_{\text{Nd}}(t)$  值(-5.8~-5.2), Pb 同位素的  $^{206}\text{Pb}/^{204}\text{Pb}$  为 18.6091~18.6438,  $^{207}\text{Pb}/^{204}\text{Pb}$  为 15.6900~15.6986,  $^{208}\text{Pb}/^{204}\text{Pb}$  为 39.2116~39.2225, 指示岩浆可能为特提斯洋俯冲消减阶段产生的岛弧地幔楔部分熔融的产物。一种可能的成因模式为: 晚白垩世, 随着雅鲁藏布江板块向拉萨地块之下俯冲, 俯冲板片流体交代上覆地幔楔, 形成幔源基性岩浆, 上侵到地壳后, 诱发了岛弧基底物质的部分熔融, 形成了中基性的纳如松多石英闪长岩, 其形成可能是晚白垩世北向俯冲的新特提斯洋板块在回转初期的岩浆活动响应。

**关键词** 地球化学; 晚白垩世; 石英闪长岩; 纳如松多矿床; 西藏

中图分类号:P618.42; P618.43

文献标志码:A

## Petrogenesis of quartz diorites of Narusongduo Pb-Zn deposit, Tibet: Constraints from geochemistry and Sr-Nd-Pb isotopes

GONG XueJing<sup>1</sup>, YANG ZhuSen<sup>2</sup>, ZHUANG LiangLiang<sup>3</sup> and MA Wang<sup>4</sup>

(1 China Deep Exploration Center—SinoProbe Center, Chinese Academy of Geological Sciences, Beijing 100037, China; 2 MNR Key Laboratory and Mineral Assessment, Institute of Mineral Resources, Chinese Academy of Geological Sciences, Beijing 100037, China;

3 School of Earth Sciences and Resources, China University of Geosciences, Beijing 100083, China; 4 Institute of Geology,  
Chinese Academy of Geological Sciences, Beijing 100037, China)

### Abstract

The Late Cretaceous quartz diorite containing 10%~15% amphibole in Narusongduo Pb-Zn deposit with characteristics of low content of  $\text{SiO}_2$  and high content of  $\text{MgO}$  and  $\text{CaO}$  is aluminous I-type granite with low degree of differentiation, belongs to high potassium calc alkaline to shoshonite series. The rock is characterized by weakly developed Eu negative anomaly, enrichment of strong incompatible elements such as Rb, Th and U, and depletion of Nb, Ta, Ti and other high field strength elements. The isotope analyses show that the Narusongduo quartz diorite has a relatively high  $^{87}\text{Sr}/^{86}\text{Sr}$  initial ratios (0.709 13~0.709 68) and negative  $\varepsilon_{\text{Nd}}$  values (-5.8~-5.2), with the lead isotope ratio of  $^{206}\text{Pb}/^{204}\text{Pb}$  being 18.6091~18.6438,  $^{207}\text{Pb}/^{204}\text{Pb}$  being 15.6900~15.6986, and  $^{208}\text{Pb}/^{204}\text{Pb}$  being 39.2116~39.2225. The geochemical and isotopic geochemical studies show that the magma might have originated from

\* 本文得到国家重点研发计划“深地资源勘查开采”重点专项(编号:2016YFC0600306)和地质调查项目(编号:DD20179172)的联合资助

第一作者简介 龚雪婧,女,1988 年生,博士,助理研究员,主要从事岩石地球化学及矿床学研究。Email: xuejinggong@cags.ac.cn

\*\* 通讯作者 杨竹森,男,1964 年生,博士,研究员,从事矿床学及矿床地球化学研究。Email: yangzhusen@vip.sina.com

收稿日期 2018-03-19; 改回日期 2018-12-01。秦思婧编辑。

the partial melting of the island arc mantle wedge produced during the subduction of the Tethys Ocean. A possible genetic model is as follows: In the Late Cretaceous, along with the subduction of Yarluzangbo Plate beneath the Lhasa block, the subducting slab fluid metasomatized the overlying mantle wedge, forming the mantle-derived magma. The ascending emplacement of the mantle-derived magma induced partial melting of the island arc basement material and formed the Narusongduo quartz diorites. The formation was probably the magmatic response to the rolling-back of the northern subducting Neo-Tethys Oceanic Plate in Late Cretaceous.

**Key words:** geochemistry, Late Cretaceous, quartz diorites, Narusongduo deposit, Tibet

青藏高原所包含的广大地区,先后经历了原特提斯、古特提斯、新特提斯与印-亚大陆碰撞等多个阶段的地质事件,并伴随有多期、多成因的花岗岩类产出和大规模成矿作用的发生,形成冈底斯巨型斑岩铜矿带(涂光炽等,1981;江万等,1999;莫宣学等,2003; 2005; 2006; 侯增谦等,2004; 2006a; 2009; 2012; 孟祥金等,2007; 张宏飞等,2007; 杨志明等,2008a; 2011; Zhu et al., 2011; 王保弟等,2013)和其北侧的银铅锌多金属成矿带(Leach et al., 2005; 藏文栓等,2007; 唐菊兴等,2009; 高一鸣等,2009; 2011a; 2011b; 王立强等,2011; 2012; 2014; 黄克贤等,2012; Hou et al., 2015; 付强等,2014; 2015; Zheng et al., 2015; Fu et al., 2017)。纳如松多铅锌矿床作为冈底斯银铅锌多金属成矿带内的典型矿床之一,吸引了众多的研究者,研究工作主要集中在成矿岩体的形成时代和元素地球化学方面(杨勇等,2010a; 纪现华等,2012),以及矿床地质特征、成矿时代和成矿作用等方面(杨勇等,2010b; 纪现华等,2014; 刘英超等,2015)。纪现华等(2014)利用<sup>40</sup>Ar-<sup>39</sup>Ar同位素测年方法对纳如松多东矿段隐爆角砾岩型矿体成矿阶段形成的绢云母进行了年龄测定,获得隐爆角砾岩型铅锌矿体的形成年龄为( $57.81\pm0.66$ )Ma,这一期成矿事件与矿区内地质演化密切相关;而龚雪婧等(2018)新获得矿区内地质演化特征、岩浆活动及物质来源上具有何种特征尚需研究。因此,本文在前人工作基础上,对纳如松多矿区晚白垩世石英闪长岩开展了详细的岩石地球化学和Sr-Nd-Pb同位素地球化学研究,探讨其岩浆源区特征和岩浆成因,为进一步梳理矿区内地质演化特征提供新的岩石学依据。

## 1 矿区地质概况及样品特征

西藏日喀则谢通门县纳如松多铅锌矿床位于青藏高原拉萨地块中部的隆格尔-工布江达火山岩浆弧中段(图1a),区域地质演化经历了古生代冈瓦纳大陆北缘海相沉积、中生代雅鲁藏布江洋和班公湖-怒江洋俯冲消减与闭合、新生代印度-亚洲大陆碰撞3个阶段。矿区内地层主要为下二叠统昂杰组板岩和中二叠统下拉组灰岩、古新统典中组火山岩和全新统松散堆积物。矿区内地质演化强烈,大面积分布有典中组火山岩,其为一套以中基性火山岩为主体的岩石组合,主要岩石类型为玄武岩、玄武安山岩、安山岩、英安岩、安山质凝灰熔岩、英安质(角砾)凝灰熔岩、熔结(角砾)凝灰岩、安山质(英安质)熔结火山角砾岩、英安质(含角砾)岩屑晶屑凝灰岩等,火山活动间歇或强度较弱时形成沉凝灰岩、凝灰质(粉、细)砂岩和凝灰质(砂)砾岩等。

与典中组火山岩相伴,还有中酸性侵入岩株和岩脉分布于矿区东部、中部和西南部,主要为一套中酸性岩,岩性有石英闪长岩、花岗闪长岩、细斑花岗斑岩、粗斑花岗斑岩和闪长玢岩等。石英闪长岩和花岗闪长岩呈岩株状侵入于矿区东部下二叠统昂杰组砂岩中,其中,石英闪长岩侵位稍早,呈残留体状分布于花岗闪长岩岩株西北部(图1b),其锆石U-Pb年龄为( $85.2\pm1.1$ )Ma(龚雪婧等,2018)。岩株被北西向和近东西向逆断层所切割,沿断裂发生的热液蚀变和铅锌矿化显示,石英闪长岩和花岗闪长岩岩株侵位于铅锌成矿之前,纪现华等(2014)通过矿体内成矿阶段热液绢云母<sup>40</sup>Ar-<sup>39</sup>Ar坪年龄,将成矿年龄限定为( $57.81\pm0.66$ )Ma,与笔者观察到的地质现象相符。细斑和粗斑花岗斑岩呈岩株、岩枝和岩脉状侵入于矿区中西部二叠系沉积岩和古新统火山岩中,2种斑岩间呈涌动侵入接触关系,其锆石U-Pb

年龄分别为 $(62.47\pm0.91)$  Ma 和 $(62.54\pm0.77)$  Ma(纪现华等,2012)。

本次工作采集矿区东部钻孔 ZK-2 中的新鲜石英闪长岩样品进行研究(图 2),该钻孔自上至下:① 0~3 m 为坡积砾石层;② 3~4.1 m 为绿泥石化石英闪长岩;③ 4.1~17 m 为石英闪长岩;④ 17~31.8 m 为

绿泥石化花岗闪长岩;⑤ 31.8~139 m 为石英闪长岩,石英闪长岩体中见有暗色包体。用于岩浆锆石研究的样品 ZK-2-3 采集于 39.5 m 处,为新鲜的石英闪长岩,呈灰黑色,具半自形细粒结构,块状构造,主要由斜长石、角闪石、石英及少量钾长石和黑云母组成(图 2)。斜长石含量约 55%,粒径大小不一,约 1~3

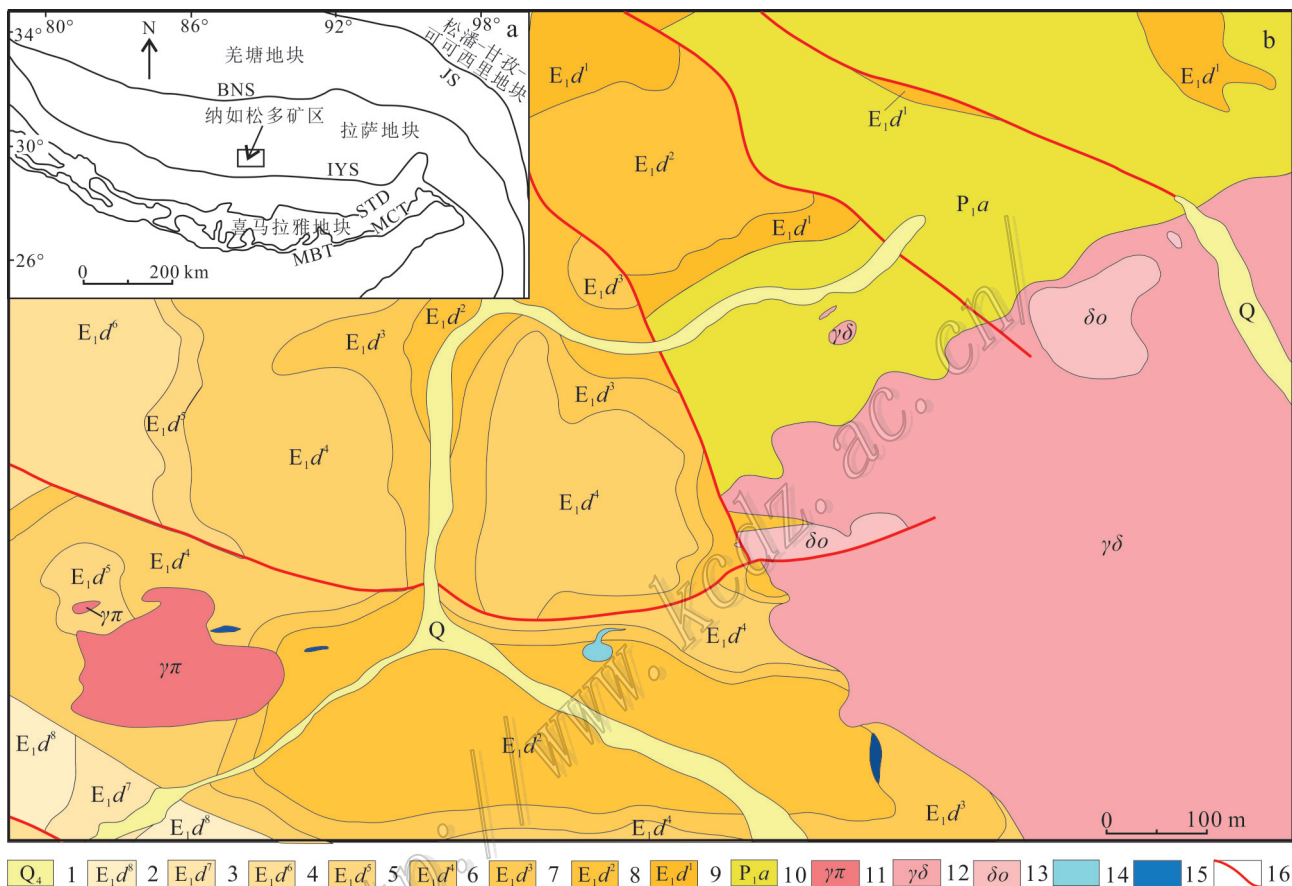


图 1 青藏高原碰撞造山带构造格架(a, 据纪现华等, 2012)及纳如松多矿区东段地质图(b, 据杨竹森未发表资料)  
1—第四系松散堆积层; 2—古新统典中组第八段安山岩; 3—古新统典中组第七段凝灰质砂砾岩; 4—古新统典中组第六段安山岩、凝灰岩;  
5—古新统典中组第五段凝灰质砂砾岩; 6—古新统典中组第四段英安岩、凝灰岩; 7—古新统典中组第三段砂砾岩;  
8—古新统典中组第二段凝灰岩; 9—古新统典中组第一段砂砾岩; 10—下二叠统昂杰组板岩; 11—花岗斑岩;  
12—花岗闪长岩; 13—石英闪长岩; 14—闪长玢岩; 15—铅锌矿体; 16—断裂

STD—藏南拆离系; MCT—主中央逆冲断裂; MBT—主边界逆冲断裂; JS—金沙江缝合线; BNS—班公湖-怒江缝合带; IYS—雅鲁藏布江缝合带

Fig. 1 Tectonic framework of the Tibetan collisional orogenic belt (a, after Ji et al., 2012) and geological map

of the eastern Narusongduo mining area( b, after unpublished material of Yang)

1—Quaternary accumulation layer; 2—8th member of Palaeocene Dianzhong Formation: andesite; 3—7th member of Palaeocene Dianzhong Formation: tuffaceous glutenite; 4—6th member of Palaeocene Dianzhong Formation: andesite and tuff; 5—5th member of Palaeocene Dianzhong Formation: tuffaceous glutenite; 6—4th member of Palaeocene Dianzhong Formation: dacite and tuff; 7—3rd member of Palaeocene Dianzhong Formation: glutenite; 8—2nd member of Palaeocene Dianzhong Formation: tuff; 9—1st member of Palaeocene Dianzhong Formation: glutenite; 10—Permian Angie Formation: slate; 11—Granite porphyry;  
12—Granodiorite; 13—Quartz diorite; 14—Diorite porphyrite; 15—Lead-zinc orebody; 16—Fracture  
STD—South Tibetan detachment system; MCT—Main central trust; MBT—Main boundary trust; JS—Jinsha river suture;  
BNS—Bangong Co-Nujiang suture; IYS—Indus-Yarlung suture

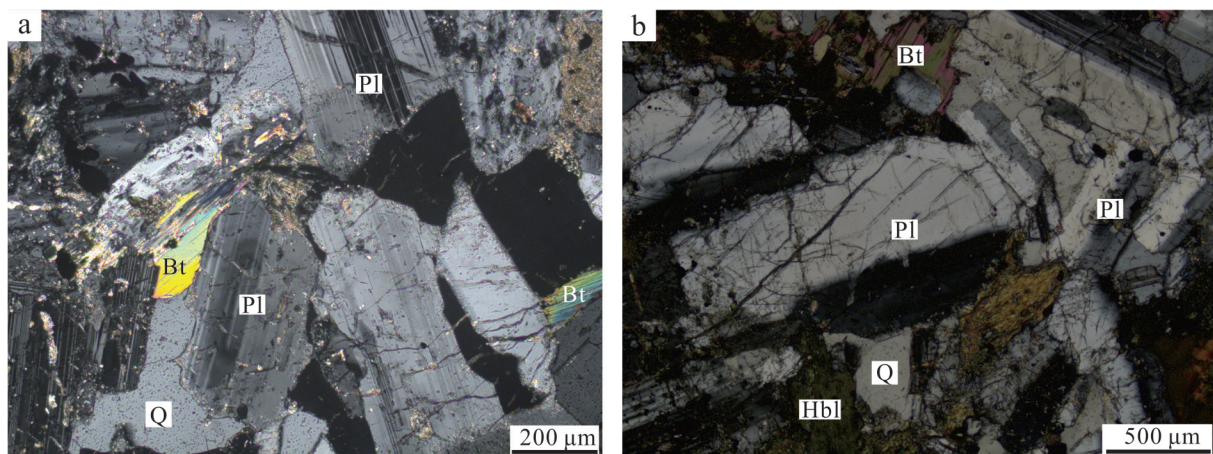


图2 纳如松多矿床石英闪长岩样品显微矿物组合特征

Pl—斜长石; Bt—黑云母; Qtz—石英; Hbl—角闪石

Fig. 2 Microscopic characteristics of the quartz diorite samples in Narusongduo deposit

Pl—Plagioclase; Bt—Biotite; Qtz—Quartz; Hbl—Hornblende

mm,呈板状,聚片双晶现象明显,偶见微弱环带结构;角闪石呈粒状、长柱状,浅黄绿色,含量约10%~15%;石英多呈他形粒状,粒径1~2 mm,含量约15%;钾长石含量约10%,黑云母含量较少,约5%,偶见绢云母化。

## 2 测试方法

主量、微量元素由国家地质实验测试中心完成。岩石样品粉碎至200目以下粉末。主量元素含量采用XRF法在X荧光光谱仪3080E测定,分析相对误差低于5%;稀土元素和微量元素采用等离子质谱(Excell)ICP-MS测定,分析相对误差低于10%。

Sr-Nd同位素测试工作在南京大学内生金属矿床成矿机制研究国家重点实验室完成,用于测量的样品溶解后采用Bio-Rad 50wx8阴离子交换树脂分离提纯后,采用Finnigan公司的Triton TI热电离质谱仪进行Sr-Nd同位素比值测量,同位素比值精度优于0.005%,具体实验流程见濮巍等,2005。

全岩Pb同位素测试工作在南京大学内生金属矿床成矿机制研究国家重点实验室完成,用于测试的样品溶解后采用HBr和阴离子交换树脂提纯后,采用Finnigan公司的Triton TI热电离质谱仪进行Pb同位素比值测量,采用国际标样NIST Pb-981进行校正,同位素比值精度优于0.05%。

## 3 分析结果

### 3.1 主量元素

纳如松多石英闪长岩主量元素分析结果见表1,  $w(\text{SiO}_2)$ 较低,为60.26%~61.50%,平均值60.66%; $w(\text{Al}_2\text{O}_3)$ 为15.57%~15.78%,平均值15.66%; $w(\text{CaO})$ 为4.61%~5.23%,平均值4.90%; $w(\text{FeO})$ 为2.86%~4.83%,平均值3.86%; $w(\text{K}_2\text{O})$ 为3.43%~4.08%,平均值3.73%; $w(\text{Na}_2\text{O})$ 为3.16%~3.42%,平均值3.31%; $w(\text{MgO})$ 为2.02%~3.22%,平均值2.71%; $w(\text{Fe}_2\text{O}_3)$ 为0.20%~2.13%,平均值1.16%; $w(\text{TiO}_2)$ 为0.92%~0.97%,平均值0.95%; $w(\text{P}_2\text{O}_5)$ 为0.27%~0.29%,平均值0.28%;全碱含量,即 $w(\text{K}_2\text{O}+\text{Na}_2\text{O})$ 为6.84%~7.24%,平均值7.04%; $\text{MgO}^{\#}$ 均大于45,范围45.46~52.12(表1)。在岩浆/火山岩系统全碱-硅(TAS)分类图(图2a)中,石英闪长岩所有投点均位于二长岩系中,结合岩石手标本及镜下观察暂且将其定名为石英闪长岩。在 $\text{K}_2\text{O}-\text{SiO}_2$ 图解(图2b)中,石英闪长岩投点落入高钾钙碱性-钾玄岩系列区域;里特曼指数( $\sigma=(\text{Na}_2\text{O}+\text{K}_2\text{O})^2/(\text{SiO}_2-43)$ )为2.71~2.89(表1),说明岩体均属于钙碱性系列。石英闪长岩铝饱和指数为0.83~0.87,显示出准铝质的特征,在ASI-SiO<sub>2</sub>图解(图2c)中,数据点均落在准铝质区域内。

### 3.2 稀土及微量元素

石英闪长岩 $\Sigma \text{REE}$ 为 $201.95 \times 10^{-6}$ ~ $243.72 \times 10^{-6}$ ,

表1 纳如松多铅锌矿床石英闪长岩主量、稀土及微量元素分析结果

Table1 Major, rare earth and trace element compositions of quartz diorite in Narusongduo Pb-Zn deposit

组分	ZK-2-3	ZK-2-4	ZK-2-5	ZK-2-6	ZK-2-7	ZK-2-8	组分	ZK-2-3	ZK-2-4	ZK-2-5	ZK-2-6	ZK-2-7	ZK-2-8
<i>w</i> (B)/%							<i>w</i> (B)/10 <sup>-6</sup>						
SiO <sub>2</sub>	60.26	60.46	61.50	61.16	60.28	60.28	Tb	0.81	0.69	0.73	0.71	0.73	0.78
TiO <sub>2</sub>	0.97	0.96	0.92	0.94	0.94	0.97	Dy	4.40	4.06	3.93	4.10	4.20	4.27
Al <sub>2</sub> O <sub>3</sub>	15.78	15.59	15.59	15.57	15.64	15.76	Ho	0.76	0.67	0.69	0.70	0.73	0.70
Fe <sub>2</sub> O <sub>3</sub>	0.20	0.40	1.64	1.29	2.13	1.27	Er	2.02	1.83	1.73	1.81	1.81	2.00
TFe <sub>2</sub> O <sub>3</sub>	5.46	5.71	5.22	4.77	5.28	5.98	Tm	0.29	0.27	0.25	0.27	0.28	0.27
FeO	4.78	4.83	3.25	3.16	2.86	4.28	Yb	1.79	1.73	1.61	1.73	1.79	1.80
MnO	0.09	0.08	0.08	0.12	0.07	0.09	Lu	0.30	0.25	0.26	0.26	0.25	0.26
MgO	2.76	3.17	2.56	2.02	2.51	3.22	Rb	161.00	188.00	154.00	179.00	187.00	151.00
CaO	5.02	4.81	4.61	4.76	5.23	4.98	Ba	551.00	573.00	497.00	574.00	563.00	525.00
Na <sub>2</sub> O	3.41	3.34	3.22	3.16	3.31	3.42	Th	25.00	25.50	26.00	27.90	24.80	23.50
K <sub>2</sub> O	3.43	3.68	4.01	4.08	3.58	3.62	U	4.51	4.13	3.93	4.35	5.18	6.15
P <sub>2</sub> O <sub>5</sub>	0.28	0.29	0.27	0.27	0.28	0.29	Nb	10.80	11.90	11.50	11.60	12.00	11.70
H <sub>2</sub> O <sup>+</sup>	1.32	1.62	1.34	1.08	1.44	1.06	Ta	0.97	0.86	0.92	0.93	0.91	0.86
LOI	1.94	1.57	1.80	3.19	2.47	1.21	Sr	630.00	608.00	529.00	642.00	588.00	545.00
Mg <sup>#</sup>	49.80	52.12	49.13	45.46	48.37	51.42	Zr	267.00	245.00	259.00	224.00	223.00	214.00
K <sub>2</sub> O+Na <sub>2</sub> O	6.84	7.02	7.23	7.24	6.89	7.04	Hf	7.56	6.27	7.23	7.84	6.09	6.06
K <sub>2</sub> O/Na <sub>2</sub> O	1.01	1.10	1.25	1.29	1.08	1.06	Y	20.10	20.00	18.50	18.60	20.70	19.60
里特曼指数	2.71	2.82	2.83	2.89	2.75	2.87	Cr	66.90	65.90	52.90	54.20	63.20	57.50
ASI	0.86	0.86	0.87	0.85	0.83	0.85	Co	17.80	17.70	15.50	15.80	17.10	17.30
<i>w</i> (B)/10 <sup>-6</sup>							Ni	43.80	40.40	34.40	35.10	39.20	37.80
La	42.50	52.70	51.80	53.80	55.40	50.40	Pb	33.30	27.00	24.20	25.10	28.50	29.20
Ce	84.10	104.00	97.60	104.00	102.00	100.00	ΣREE	201.95	239.12	230.72	239.29	243.72	233.49
Pr	10.30	12.50	12.20	12.70	12.90	12.60	LREE/HREE	10.97	14.71	14.56	14.43	14.73	13.65
Nd	39.30	45.40	45.40	44.10	48.70	45.00	La <sub>N</sub> /Yb <sub>N</sub>	17.03	21.85	23.08	22.31	22.20	20.08
Sm	7.08	7.67	7.33	7.57	7.53	7.96	δEu	0.80	0.72	0.71	0.71	0.76	0.68
Eu	1.80	1.63	1.56	1.61	1.70	1.59	δCe	0.96	0.96	0.92	0.94	0.90	0.95
Gd	6.50	5.72	5.63	5.93	5.70	5.86							

注:比值单位为1;ASI= $w(\text{Al}_2\text{O}_3)/w(\text{CaO}+\text{Na}_2\text{O}+\text{K}_2\text{O})$ 。

其中,轻稀土元素为 $185.08 \times 10^{-6}$ ~ $228.23 \times 10^{-6}$ ,重稀土元素为 $14.33 \times 10^{-6}$ ~ $16.87 \times 10^{-6}$ 之间,LREE/HREE比值为10.97~14.73(表1),稀土元素球粒陨石标准化(Sun et al., 1989)配分曲线呈右倾平滑的平行曲线簇(图4a),富集轻稀土元素,(La/Yb)<sub>N</sub>=17.03~23.08;负Eu异常中等,δEu为0.68~0.80。石英闪长岩总体上具有富集强不相容元素Rb、Th、U,而亏损高场强元素Nb、Ta、Ti的特点,显示了楔形地幔源区部分熔融的岛弧岩浆特征,应形成于俯冲带环境。相容元素含量整体偏低, $w(\text{Cr})$ 为 $52.90 \times 10^{-6}$ ~ $66.90 \times 10^{-6}$ , $w(\text{Co})$ 为 $15.50 \times 10^{-6}$ ~ $17.80 \times 10^{-6}$ , $w(\text{Ni})$ 为 $34.40 \times 10^{-6}$ ~ $43.80 \times 10^{-6}$ , $w(\text{Pb})$ 为 $24.20 \times 10^{-6}$ ~ $33.30 \times 10^{-6}$ ,较高的*w*(Pb)说明岩浆

受到了地壳物质的影响。

### 3.3 Sr-Nd-Pb同位素组成

石英闪长岩具有较高的*w(Rb)*和极高的*w(Sr)*,分别为 $141 \times 10^6$ ~ $151 \times 10^6$ 和 $545 \times 10^6$ ~ $630 \times 10^6$ ,(<sup>87</sup>Sr/<sup>86</sup>Sr)<sub>i</sub>为0.70913~0.70968(表2)。Sr初始值与由地幔形成玄武质岩浆的Sr初始值(0.706)相比要大,但比地壳部分熔融形成花岗岩的Sr初始值(0.718)偏小,暗示岩浆形成或演化过程中可能存在不同地球化学端元的加入。纳如松多石英闪长岩ε<sub>Nd</sub>值较低,为-5.8~5.2(表2)。石英闪长岩Pb同位素的<sup>206</sup>Pb/<sup>204</sup>Pb为18.6091~18.6438,<sup>207</sup>Pb/<sup>204</sup>Pb为15.6900~15.6986,<sup>208</sup>Pb/<sup>204</sup>Pb为39.2116~39.2225(表3)。

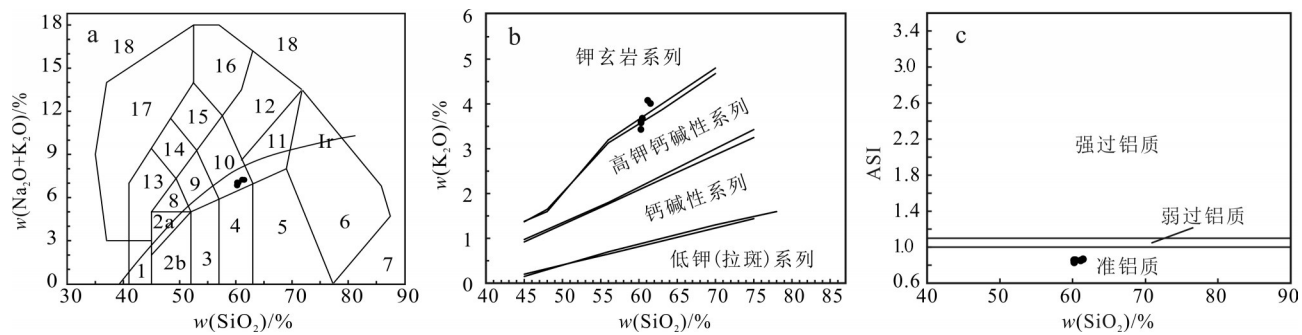


图3 岩石类型和系列划分图解

a.  $\text{SiO}_2-(\text{Na}_2\text{O}+\text{K}_2\text{O})$  图解(分类据 Wilson, 1989); 1—橄榄辉长岩; 2a—碱性辉长岩; 2b—亚碱性辉长岩; 3—辉长闪长岩; 4—闪长岩; 5—花岗闪长岩; 6—花岗岩; 7—硅英岩; 8—二长辉长岩; 9—二长闪长岩; 10—二长岩; 11—石英二长岩; 12—正长岩; 13—副长石辉长岩; 14—副长石二长闪长岩; 15—副长石二长正长岩; 16—副长石正长岩; 17—副长石深成岩; 18—霓方钠岩/磷霞岩/粗白榴岩); b.  $\text{SiO}_2-\text{K}_2\text{O}$  图解(据 Le Maitre, 2002); c. ASI- $\text{SiO}_2$  图解

Fig. 3 Classification and serial diagrams of the granitoids

a.  $\text{SiO}_2-(\text{Na}_2\text{O}+\text{K}_2\text{O})$  diagram (after Wilson, 1989; 1—Olivine gabbro; 2a—Alkaline gabbro; 2b—Subalkaline gabbro; 3—Gabbro diorite; 4—Diorite; 5—Granodiorite; 6—Granite; 7—Quartzolite; 8—Monzogabbro; 9—Monzodiorite; 10—Monzonite; 11—Adamellite; 12—Syenite; 13—Parafeldspar gabbro; 14—Parafeldspar monzodiorite; 15—Foid monzosyenite; 16—Parafeldspar syenite; 17—Parafeldspar plutonic rocks; 18—Tawite/ urtite/ italite); b.  $\text{SiO}_2-\text{K}_2\text{O}$  diagram (after Le Maitre, 2002); c. ASI- $\text{SiO}_2$  diagram

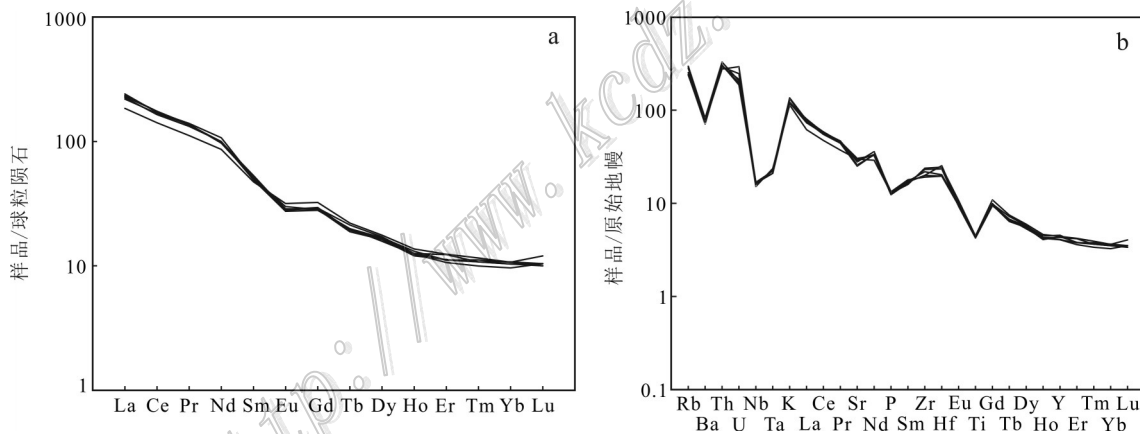


图4 稀土元素球粒陨石标准化配分曲线图(a)和微量元素原始地幔标准化配分曲线图(b,球粒陨石、原始地幔数据据 Sun et al., 1989)

Fig. 4 Chondrite-normalized REE patterns (a) and primitive mantle-normalized trace element patterns (b, data of chondrite and primitive mantle after Sun et al., 1989)

## 4 讨 论

### 4.1 岩石成因

纳如松多石英闪长岩样品具有低  $\text{SiO}_2$ 、高  $\text{MgO}$ 、高  $\text{CaO}$  的特征, 显著区别于典型的 A型花岗岩 (Frost et al., 2001; Clemens, 2003; Miller, 1985; Miller et al., 2003), 且在 A型花岗岩判别图解(图 5a、b)中, 石英闪长岩样品基本落入未分异的 I/S型花岗岩区内。

域内, 结合岩体的形成时代为 85.2 Ma, 处于雅鲁藏布江洋北向俯冲的构造演化阶段 (莫宣学等, 2006), 排除了石英闪长岩为 A型花岗岩的可能。在对石英闪长岩进行的岩相学研究中, 发现其含有 10%~15% 的角闪石, 而并未在岩体中观察到白云母、石榴子石及堇青石等富铝矿物, 直观地说明石英闪长岩为 I型花岗岩 (Chappell, 1999)。在  $\text{K}_2\text{O}-\text{Na}_2\text{O}$  图解(图 5c)中, 石英闪长岩落入 I型花岗岩区域内。另外, 石英闪长岩的  $\text{Sr}/\text{Ba}$  比值介于 1.01~1.14, 与刘振声等

表2 纳如松多铅锌矿床石英闪长岩Sr-Nd同位素分析结果

Table 2 Sr-Nd isotope compositions of quartz diorite in Narusongduo Pb-Zn deposit

样品号	$w(B)/10^{-6}$		$^{87}\text{Rb}/^{86}\text{Sr}$	$^{87}\text{Sr}/^{86}\text{Sr}$	$(^{87}\text{Sr}/^{86}\text{Sr})_t$	$w(B)/10^{-6}$		$(^{143}\text{Nd}/^{144}\text{Nd})_t$	$\varepsilon_{\text{Nd}}(t)$
	Rb	Sr				Sm	Nd		
ZK-2-3	161	630	0.6368	0.7098	0.70968	7.08	39.3	0.1089	0.5123
ZK-2-8	151	545	0.6904	0.7093	0.70913	7.96	45	0.1069	0.5122

表3 纳如松多铅锌矿床石英闪长岩Pb同位素分析结果

Table 3 Pb isotope compositions of quartz diorite in Narusongduo Pb-Zn deposit

样品号	岩性	$^{206}\text{Pb}/^{204}\text{Pb}$	$1\sigma$	$^{207}\text{Pb}/^{204}\text{Pb}$	$1\sigma$	$^{208}\text{Pb}/^{204}\text{Pb}$	$1\sigma$
ZK-2-3	石英闪长岩	18.6091	0.0006	15.6986	0.0005	39.2116	0.0012
ZK-2-8	石英闪长岩	18.6438	0.0007	15.6900	0.0006	39.2225	0.0016

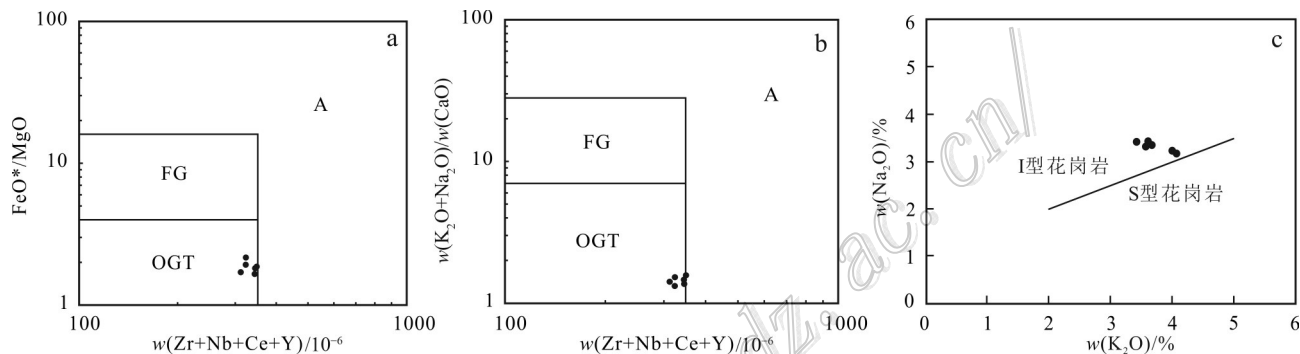


图5 纳如松多石英闪长岩成因类型判别图(a,b,底图据Whalen et al., 1987; c,底图据Chappell, 1999)

FG—分异的长英质花岗岩; OGT—未分异的I、S型花岗岩; A—A型花岗岩

Fig. 5 Genetic type discrimination diagrams of quartz diorite from Narusongduo Pb-Zn deposit

(a, b, base map after Whalen et al., 1987; c, base map after Chappell, 1999)

FG—Fractionated felsic granites; OGT—Unfractionated M-, I- and S-type granites; A—A-type granites

(1994)总结的I型花岗岩相对富集Sr, Sr/Ba比值一般大于0.5,而S型花岗岩相对富集Ba, Sr/Ba比值一般小于0.5的特征相符。综上所述,纳如松多矿区石英闪长岩为分异程度较低的I型花岗岩。

前人研究显示,I型花岗岩由壳内中基性火成岩或变质岩部分熔融而来(Chappell et al., 1988; 吴福元等,2007),或者地壳重融过程中,幔源贡献量增加形成(Kemp et al., 2007; Collins et al., 2008; 李献华等,2009)。纳如松多矿区石英闪长岩样品具有富集轻稀土元素和大离子亲石元素(Rb、Th、U)、亏损高场强元素(Nb、Ta、Ti)的地球化学特征,这表明源区可能是古老下地壳或受俯冲板片流体或熔体交代的富集岩石圈地幔。此外,这些石英闪长岩( $^{87}\text{Sr}/^{86}\text{Sr}$ )值为0.709 13~0.709 68,具有负的全岩 $\varepsilon_{\text{Nd}}(t)$ 值(-5.8~-5.2)和较高的 $\varepsilon_{\text{Hf}}(t)$ 值(-1.44~1.70)(龚雪婧等,2018),均显示出了富集源区的性质,且源区组成较均一。在Sr-Nd同位素相关图(图6a)

中,Sr-Nd同位素组成靠近EM II富集地幔端员,暗示源区有消减物质(洋壳携带的沉积物或洋壳板片熔体)加入到了地幔源区;在 $^{206}\text{Pb}/^{204}\text{Pb}$ - $^{207}\text{Pb}/^{204}\text{Pb}$ 图解(图6b)中,样品点同样靠近EM II富集地幔特征区域。此外,纳如松多石英闪长岩具有较低的Mg<sup>#</sup>和相容元素含量,较低的Nb/U(1.90~2.93)和Ce/Pb(2.53~4.14)比值,与全球平均大洋沉积物(GLOSS)的比值(Nb/U=5.3和Ce/Pb=2.9, Plank et al., 1998)接近,明显不同于洋中脊和洋岛玄武岩(Nb/U=47和Ce/Pb=27, Hofmann et al., 1986),指示纳如松多石英闪长岩可能为特提斯洋俯冲消减阶段产生的岛弧地幔楔部分熔融的产物。

#### 4.2 地球动力学背景

在微量元素原始地幔标准化蛛网图(图4b)中可以看到,石英闪长岩明显富集Rb、Th、U、K等大离子亲石元素,亏损Nb、Ta、Ti等高场强元素,其配分模式具有明显的Nb-Ta槽和Ti谷,表现出与俯冲相关

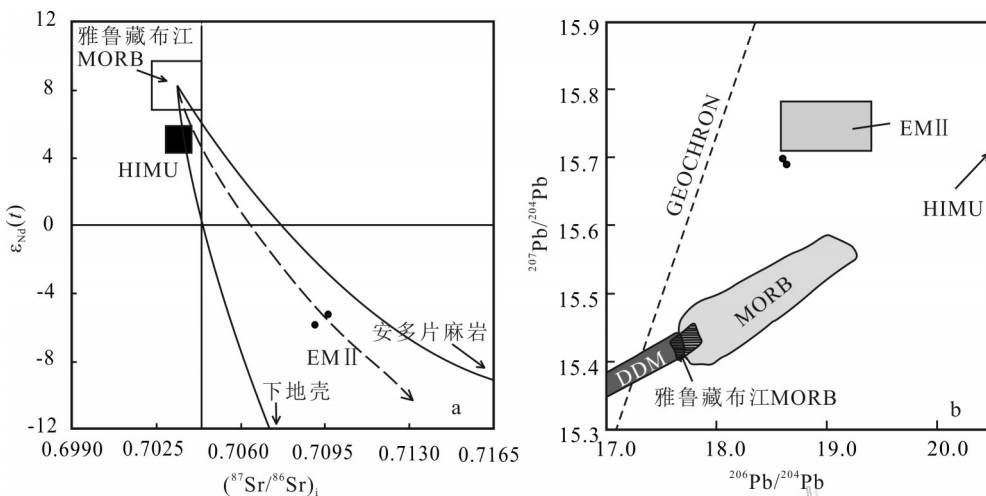


图6 纳如松多晚白垩世石英闪长岩 $\epsilon_{\text{Nd}}(t)$ - $(^{87}\text{Sr}/^{86}\text{Sr})_i$ (a, 底图据杨勇, 2010) 及 $^{206}\text{Pb}/^{204}\text{Pb}$ - $^{207}\text{Pb}/^{204}\text{Pb}$ (b, 底图据李晓雄等, 2015) 图解

HIMU—高μ地幔; EM II—富集地幔Ⅱ; DDM—亏损地幔; MORB—大洋中脊玄武岩

Fig. 6  $^{87}\text{Sr}/^{86}\text{Sr}$  versus  $\epsilon_{\text{Nd}}(t)$  diagram (a, base map after Yang, 2010) and  $^{206}\text{Pb}/^{204}\text{Pb}$  versus  $^{207}\text{Pb}/^{204}\text{Pb}$

(b, base map after Li et al., 2015) showing the isotope signatures for the Narusongduo quartz diorite  
HIMU—High μ Mantle; EM II—Enriched mantle type Ⅱ; DDM—Depleted mantle; MORB—Mid-Ocean ridge basalt

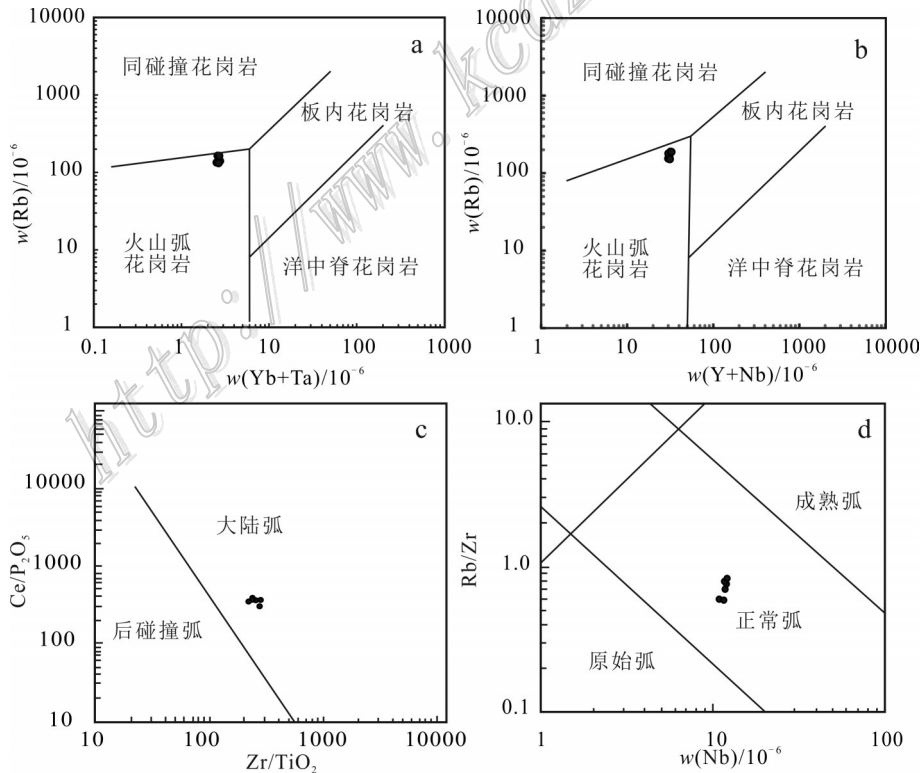


图7 纳如松多石英闪长岩构造环境判别图解

(a、b, 底图据 Pearce et al., 1984; c, 底图据 Müller et al., 1992; d, 底图据 Brown et al., 1984)

Fig. 7 Tectonic setting discrimination diagrams of quartz diorite from Narusongduo Pb-Zn deposit

(a, b, base map after Pearce et al., 1984; c, base map after Müller et al., 1992; d, base map after Brown et al., 1984)

的弧花岗岩的特征(Rogers et al., 1989; Stern, 2002),表明岩浆的源区曾经历了板片释放流体的交代(Miller et al., 1999; Wang et al., 2001; Hou et al., 2004; 杨志明等, 2008a; 2008b)。在花岗岩类构造环境判别图(图7a、b)中,石英闪长岩样品均投点于弧花岗岩范围内,同样说明其形成与俯冲作用相关。在Zr/TiO<sub>2</sub>-Ce/P<sub>2</sub>O<sub>5</sub>图解(图7c)中,样品点均落入大陆弧范围内,由此推测石英闪长岩为产出在活动大陆边缘的陆缘弧岩浆岩,这也与纳如松多矿区位于中拉萨地体与南拉萨地体过渡带的地质事实相符。在Nb-Rb/Zr图解(图7d)中,投点均位于正常弧范围,暗示石英闪长岩为俯冲带原始岛弧演化到正常弧环境的岩浆产物(Brown, 1984)。

Ji等(2009)认为205 Ma左右和109~80 Ma的冈底斯带岩浆活动都与新特提斯洋北向俯冲的“安第斯型”稳定的岛弧俯冲作用有关,其后,在晚白垩世(约100~90 Ma),北向俯冲的新特提斯洋壳俯冲角度变小(Wen et al., 2008; Zhang et al., 2010),该时期的俯冲带前缘造山作用造成拉萨地块晚白垩世地壳的缩短、抬升与变形(Yin et al., 2000; Kapp et al., 2007; Leier et al., 2007)。在晚白垩世(90~55 Ma),低角度北向俯冲的新特提斯洋板片由于重力原因在90 Ma左右发生回转,拖拽大陆板片向下俯冲到较深位置,导致陆-陆汇聚速率加快(Chung et al., 2005; 侯增谦等, 2006b),在这个过程中上涌的软流圈提供热量,使俯冲的新特提斯洋板片熔体及流体交代上覆地幔楔。结合纳如松多石英闪长岩的地球化学特征,笔者倾向性地认为,这一过程形成的幔源基性岩浆上侵到地壳后,诱发了岛弧基底物质的部分熔融,形成了中基性的纳如松多石英闪长岩,其形成可能是晚白垩世北向俯冲的新特提斯洋板块在回转初期的岩浆活动响应。

## 5 结 论

(1) 石英闪长岩具有低SiO<sub>2</sub>、富MgO和CaO的特征,且含有10%~15%的角闪石,为准铝质、分异程度较低的高钾钙碱性-钾玄岩系列I型花岗岩。明显富集Rb、Th、U、K等大离子亲石元素,亏损Nb、Ta、Ti等高场强元素,其配分模式具有明显的Nb-Ta槽和Ti谷,表现出与俯冲相关的弧花岗岩的特征。

(2) 石英闪长岩Sr-Nd-Pb同位素成分特征显示

岩浆源区有消减物质(洋壳携带的沉积物或洋壳板片熔体)加入到了地幔源区,结合其较低的Mg<sup>#</sup>、相容元素含量和Nb/U、Ce/Pb比值,分析其可能起源于特提斯洋俯冲消减阶段产生的岛弧地幔楔的部分熔融的产物,其形成可能是晚白垩世北向俯冲的新特提斯洋板块在回转初期的岩浆活动响应。

**致 谢** 野外工作中得到了西藏宝翔矿业有限公司工作人员的大力支持,中国地质科学院地质研究所的曹康博士对文章的讨论部分提出了大量建设性意见,审稿人对本文进行了详细的审阅并提出了宝贵的修改建议,在此一并表示衷心的感谢。

## References

- Brown C G, Thorpe R S and Webb P C. 1984. The geochemical characteristics of granitoids in contrasting arcs and comments on magma sources[J]. Journal of the Geological Society, 141(3): 411-426.
- Chappell B W and Stephens W E. 1988. Origin of infracrustal (I-type) granite magmas[J]. Earth and Environmental Science Transactions of the Royal Society of Edinburgh, 79(2): 71-86.
- Chappell B W. 1999. Aluminium saturation in I-and S-type granites and the characterization of fractionated haplogranites[J]. Lithos, 46(3): 535-551.
- Chung S L, Chu M F, Zhang Y Q, Xie Y W, Lo C H, Lee T Y, Lan C Y, Li X H, Zhang Q and Wang Y Z. 2005. Tibetan tectonic evolution inferred from spatial and temporal variations in post-collisional magmatism[J]. Earth Science Review, 68(3-4): 173-196.
- Clemens J D. 2003. S-type granitic magmas-petrogenetic issues, models and evidence[J]. Earth Science Review, (61): 1-18.
- Collins W J and Richards S W. 2008. Geodynamic significance of S-type granites in circum-Pacific orogens[J]. Geology, 36: 559-562.
- Frost B R, Barnes C G, Collins W J, Arculus R J, Ellis D J and Frost C D. 2001. A geochemical classification of granitic rocks[J]. Journal of Petrology, 42(11): 2033-2048.
- Fu Q, Yang Z S, Zheng Y C, Huang K X and Duan L F. 2014. Ar-Ar age of phlogopite from the Longmala copper-iron-lead-zinc deposit in Tibet and its geodynamic significance[J]. Acta Petrologica et Mineralogica, 33(2): 283-293(in Chinese with English abstract).
- Fu Q, Huang K X, Zheng Y C, Yang Z S and Duan L F. 2015. Ar-Ar age of muscovite from skarn orebody of the Mengya'a lead-zinc deposit in Tibet and its geodynamic significance[J]. Acta Geologica Sinica, 89(3): 569-582(in Chinese with English abstract).
- Fu Q, Xu B, Zheng Y C, Yang Z S, Hou Z Q, Huang K X, Liu Y C, Zhang C and Zhao L. 2017. Two episodes of mineralization in the Mengya'a deposit and implications for the evolution and intensity of Pb-Zn-(Ag) mineralization in the Lhasa terrane, Tibet[J]. Ore

- Geology Reviews, 90: 877-896.
- Gao Y M, Chen Y C, Tang J X, Du X, Li X F, Gao M and Cai Z C. 2009. SHRIMP U-Pb dating of zircon from quartz porphyry in the Yaguila Pb-Zn-Mo deposit, Gongbujiangda County, Tibet and its geological implication[J]. *Acta Geologica Sinica*, 83(10): 1437-1444(in Chinese with English abstract).
- Gao Y M, Chen Y C, Tang J X, Li C, Li X F, Gao M and Cai Z C. 2011a. Re-Os dating of molybdenite from the Yaguila porphyry molybdenite deposit in Gongbo'gyamda area, Tibet, and its geological significance[J]. *Geological Bulletin of China*, 30(7): 1027-1036 (in Chinese with English abstract).
- Gao Y M, Chen Y C, Wang C H and Hou K J. 2011b. Zircon Hf isotopic characteristics and constraints on petrogenesis of Mesozoic-Cenozoic magmatic rocks in Nyainqntanglha region, Tibet[J]. *Mineral Deposits*, 30(2): 279-291(in Chinese with English abstract).
- Gong X J, Yang Z S, Zhao X Y, Zhang X and Guan W Q. 2018. Formation mechanism of Late Cretaceous intrusive rocks in Narusongduo Pb-Zn deposit, Tibet: Evidence from magmatic zircon[J]. *Mineral Deposits*, 37(1):91-104 (in Chinese with English abstract).
- Hofmann A, Jochum K, Seufert M and White M. 1986. Nb and Pb in oceanic basalts: New constraints on mantle evolution[J]. *Earth and Planetary Science Letters*, 33:33-45.
- Hou Z Q, Gao Y F, Meng X J, Qu X M and Huang W. 2004. Genesis of adakitic porphyry and tectonic controls on the Gangdese Miocene porphyry copper belt in the Tibetan orogeny[J]. *Acta Petrologica Sinica*, 20(2): 239-248(in Chinese with English abstract).
- Hou Z Q, Gao Y F, Qu X M, Rui Z Y and Mo X X. 2004. Origin of adakitic intrusives generated during mid-Miocene east-west extension in southern Tibet[J]. *Earth and Planetary Science Letters*, 220: 139-155.
- Hou Z Q, Yang Z S, Xu W Y, Mo X X, Ding L, Gao Y F, Dong F L, Li G M, Qu X M, Zhao Z D, Jiang S H, Meng X J, Li Z Q, Qin K Z and Yang Z M. 2006a. Metallogenesis in Tibetan collisional orogenic belt: I . Mineralization in main collisional orogenic setting [J]. *Mineral Deposits*, 25(4): 337-358(in Chinese with English abstract).
- Hou Z Q, Mo X X, Gao Y F, Yang Z M, Dong G C and Ding L. 2006b. Early processes and tectonic model for the Indian-Asian continental collision: Evidence from the Cenozoic Gangdese igneous rocks in Tibet[J]. *Acta Geologica Sinica*, 80(9): 1233-1248(in Chinese with English abstract).
- Hou Z Q and Yang Z M. 2009. Porphyry deposits in continental settings of China: Geological characteristics, magmatic-hydrothermal system, and metallogenic model[J]. *Acta Geologica Sinica*, 83 (12): 1780-1817(in Chinese with English abstract).
- Hou Z Q, Zheng Y C, Yang Z M and Yang Z S. 2012. Metallogenesis of continental collision setting: Part I . Gangdese Cenozoic porphyry Cu-Mo systems in Tibet[J]. *Mineral Deposits*, 31(4): 647-670(in Chinese with English abstract).
- Hou Z Q, Duan L F, Lu Y J, Zheng Y C, Zhu D C, Yang Z M, Yang Z S, Wang B D, Pei Y R, Zhao Z D and McCuaig T C. 2015. Lithospheric architectures of the Lhasa Terrane and its control on ore deposits in Himalayan-Tibetan orogeny[J]. *Economic Geology*, 110: 1541-1575.
- Huang K X, Zheng Y C, Zhang S, Li W, Sun Q Z, Li Q Y, Liang W, Fu Q and Hou Z Q. 2012. LA-ICP-MS zircon U-Pb dating of two types of porphyry in the Yaguila mining area, Tibet[J]. *Acta Petrologica et Mineralogica*, 31(3): 348-360(in Chinese with English abstract).
- Ji W Q, Wu F Y, Chong S L, Li J X and Liu C Z. 2009. Zircon U-Pb geochronology and Hf isotopic constraints on petrogenesis of the Gangdese batholith, southern Tibet[J]. *Chemical Geology*, 262(3-4): 229-245.
- Ji X H, Yang Z S, Yu Y S, Shen J F, Tian S H, Meng X J, Li Z Q and Liu Y C. 2012. Formation mechanism of magmatic rocks in Narusongduo lead-zinc deposit of Tibet: Evidence from magmatic zircon[J]. *Mineral Deposits*, 31(4): 758-774(in Chinese with English abstract).
- Ji X H, Meng X J, Yang Z S, Zhang Q, Tian S H, Li Z Q, Liu Y C and Yu Y S. 2014. The Ar-Ar geochronology of sericite from the cryptoeexplosive breccias type Pb-Zn deposit in Narusongduo and its significance[J]. *Geology and Prospecting*, 50(2): 281-290(in Chinese with English abstract).
- Jiang W, Mo X X, Zhao C H, Guo T Y and Zhang S Q. 1999. Geochemistry of granitoid and its mafic microgranular enclave in Gangdese belt, Qinghai-Xizang Plateau[J]. *Acta Petrologica Sinica*, 15(1): 89-97(in Chinese with English abstract).
- Kapp P, DeCelles P G, Leier A L, Fabijanic J M, He S D, Pullen A and Gehrels G E. 2007. The Gangdese retroarc thrust belt revealed[J]. *GSA Today*, 17(7): 4-9.
- Kemp A I S, Hawkesworth C J, Foster G L, Paterson B A, Woodhead J D, Hergt J M, Gray C M and Whitehouse M J. 2007. Magmatic and crustal differentiation history of granitic rocks from Hf-O isotopes in zircon[J]. *Science*, 16: 980-983.
- Le Maitre R W. 2002. Igneous rocks: A classification and glossary of terms[M]. 2<sup>nd</sup> Edition. Cambridge University Press. 1-256.
- Leach D L, Sangster D F, Kelly K D, Large R, Garven G, Allen C R, Gutzmer J and Walters S. 2005. Sediment-hosted lead-zinc deposits: A global perspective[J]. *Economic Geology* 100<sup>th</sup> Anniversary Volume, 561-607.
- Leier A L, DeCelles P G, Kapp P and Ding L. 2007. The takena formation of the Lhasa terrane, southern Tibet: The record of a Late Cretaceous retroarc foreland basin[J]. *Geological Society of America Bulletin*, 119(1-2): 31-48.
- Li X H, Li W X, Wang X C, Li Q L, Liu Y and Tang G Q. 2009. Role of mantle-derived magma in genesis of early Yanshanian granites in the Nanling Range, South China: In situ zircon Hf-O isotopic constraints[J]. *Science in China (Series D-Earth Sciences)*, 39(7): 872-887(in Chinese with English abstract).
- Li X X, Jiang W, Liang J H, Zhao Z D, Liu D and Mo X X. 2015. The geochemical characteristics and significance of the basalt from

- Shexing Formation in Linzhou basin, southern Tibet[J]. *Acta Petrologica Sinica*, 31(5): 1285-1297(in Chinese with English abstract).
- Liu Y C, Ji X H, Hou Z Q, Tian S H, Li Z Q, Zhao X Y, Zhou J S, Ma W and Yang Z S. 2015. The establishment of an independent Pb-Zn mineralization system related to magmatism: A case study of the Narusongduo Pb-Zn deposit in Tibet[J]. *Acta Petrologica et Mineralogica*, 34(4): 539-556(in Chinese with English abstract).
- Liu Z S and Wang J M. 1994. Geological geochemistry of granites in the southern Tibetan Plateau[M]. Chengdu: Sichuan Science and Technology Press. 1-133.
- Meng X J, Hou Z Q, Ye P S, Yang Z S, Li Z Q and Gao Y F. 2007. Characteristics and ore potentiality of Gangdese silver-polymetallic mineralization belt in Tibet[J]. *Mineral Deposits*, 26(2): 153-162(in Chinese with English abstract).
- Miller C F. 1985. Are strongly peraluminous magmas derived from politic sedimentary sources[J]. *Journal of Geology*, 93(6): 673-689.
- Miller C, Schuster R, Klotzli U, Frank W and Purtscheller F. 1999. Post-collisional potassic and ultrapotassic magmatism in SW Tibet: Geochemical and Sr-Nd-Pb-O isotopic constraints for mantle source characteristics and petrogenesis[J]. *Journal of Petrology*, 40: 1399-1424.
- Miller C F, McDowell S M and Mapes R W. 2003. Hot and cold granites? Implications of zircon saturation temperatures and preservation of inheritance[J]. *Geology*, 31(6): 529-532.
- Mo X X, Zhao Z D, Deng J F, Dong G C, Zhou S, Guo T Y, Zhang S Q and Wang L L. 2003. Response of volcanism to the India-Asia collision[J]. *Earth Science Frontiers*, 10(3): 135-148(in Chinese with English abstract).
- Mo X X, Dong G C, Zhao Z D, Zhou S, Wang L L, Qiu R Z and Zhang F Q. 2005. Spatial and Temporal distribution and characteristics of granitoids in the Gangdese, Tibet and implication for crustal growth and evolution[J]. *Geological Journal of China Universities*, 11(3): 281-290(in Chinese with English abstract).
- Mo X X and Pan G T. 2006. From the Tethys to the formation of the Qinghai Tibet Plateau: Constrained by tectono magmatic events[J]. *Earth Science Frontiers*, 13(6): 43-51(in Chinese with English abstract).
- Müller D, Rock N M S and Groves D I. 1992. Geochemical discrimination between shoshonitic and potassic volcanic rocks in different tectonic settings: A pilot study[J]. *Mineralogy and Petrology*, 46 (4): 259-289.
- Pearce J A, Harris N B W and Tiggle A G. 1984. Trace element discrimination diagrams for the tectonic interpretation of granitic rocks[J]. *Journal of Petrology*, 25:956-983.
- Plank T and Langmuir C H. 1998. The chemical composition of subducting sediment and its consequences for the crust and mantle[J]. *Chemical Geology*, 145(3-4): 325-394.
- Pu W, Gao J F, Zhao K D, Ling H F and Jiang S Y. 2005. Separation method of Rb-Sr, Sm-Nd using DCTA and HIBA[J]. *Journal of Nanjing University(Natural Sciences)*, 41(4): 445-450(in Chinese with English abstract).
- Rogers G and Hawkesworth C J. 1989. A geochemical traverse across the North Chilean Andes: Evidence for crust generation from the mantle wedge[J]. *Earth and Planetary Science Letters*, 91(3-4): 271-285.
- Stern R J. 2002. Subduction zones[J]. *Reviews of Geophysics*, 40(4): 1-38.
- Sun S S and McDonough W F. 1989. Chemical and isotopic systematics of oceanic basalts: Implications for mantle composition and processes[A]. In: Saunders A D and Norry M J, eds. *Magmatism in the Ocean Basins*[C]. Geological Society Special Publication. 313-345.
- Tang J X, Chen Y C, Wang D H, Wang C H, Xu Y P, Qu W J, Huang W and Huang Y. 2009. Re-Os dating of molybdenite from the Sharrang porphyry molybdenite deposit in Gongbo'gyamda County, Tibet and its geological significance[J]. *Acta Geologica Sinica*, 83 (5): 698-704(in Chinese with English abstract).
- Tu G C, Zhang Y Q, Zhao Z H and Wang Z G. 1981. Characteristics and evolution of granitoids of South Tibet[J]. *Geochemica*, 1: 1-7 (in Chinese with English abstract).
- Wang B D, Xu J F, Liu B M, Chen J L, Wang L Q, Guo L, Wang D B and Zhang W P. 2013. Geochronology and ore-forming geological background of ~90 Ma porphyry copper deposit in the Lhasa Terrane, Tibet Plateau[J]. *Acta Geologica Sinica*, 87(1): 71-80(in Chinese with English abstract).
- Wang J H, Yin A, Harrison T M, Grove M, Zhang Y Q and Xie G H. 2001. A tectonic model for Cenozoic igneous activities in the eastern Indo-Asian collision zone[J]. *Earth and Planetary Science Letters*, 188: 123-133.
- Wang L Q, Tang J X, Chen Y C, Luo M C, Leng Q F, Chen W and Wang H. 2011. LA-ICP-MS zircon U-Pb dating of ore-bearing monzogranite porphyry in Bangpu molybdenum (copper) deposit, Tibet and its significance[J]. *Mineral Deposits*, 30(2): 349-360(in Chinese with English abstract).
- Wang L Q, Luo M C, Yuan Z H, Chen W, Leng Q F and Zhang X Q. 2012. Sulfur, lead, carbon and oxygen isotope composition and source of ore-forming materials of the Bangpu Pb-Zn ore deposit in Tibet[J]. *Acta Geoscientica Sinica*, 33(4): 435-443(in Chinese with English abstract).
- Wang L Q, Lin X, Li Z, Zhang Z, Kang H R and Li H F. 2014. Geochronology, geochemistry and Hf isotopic compositions of the granite porphyry in the Mengya'a Pb-Zn deposit, Tibet[J]. *Acta Geologica Sinica*, 88(2): 2572-2583(in Chinese with English abstract).
- Wen D R, Liu D Y, Chung S L, Chu M F, Ji J Q, Zhang Q, Song B, Lee T Y, Yeh M W and Lo C H. 2008. Zircon SHRIMP U-Pb ages of the Gangdese batholith and implications for Neotethyan subduction in southern Tibet[J]. *Chemical Geology*, 252(3-4): 191-201.
- Whalen J B, Currie K L and Chappell B W. 1987. A-type granites: Geochemical characteristics, discrimination and petrogenesis[J]. Con-

- tributions to Mineralogy and Petrology, 95(4): 407-419.
- Wilson M. 1989. Igneous petrogenesis: A global tectonic approach[M]. London: Unwin Hyman. 1-468.
- Wu F Y, Li X H, Yang J H and Zheng Y F. 2007. Discussions on the petrogenesis of granites[J]. Acta Petrologica Sinica, 23(6): 1217-1238(in Chinese with English abstract).
- Yang Y. 2010. Study on geochemical characteristics of Narusongduo silver-lead-zinc deposit, Tibet (Ph. D. thesis)[D]. Tutors: Huang Z L and Luo T Y. Guiyang: Institute of Geochemistry, Chinese Academy of Sciences(in Chinese with English abstract).
- Yang Y, Luo T Y, Yang Z S, Huang Z L, Tian S H and Qian Z K. 2010a. A comparison of porphyries between Pb-Zn-Ag metallogenetic system and Cu-Mo-Au metallogenetic system in Gangdese orogeny, Tibet[J]. Mineral Deposits, 29(2): 195-206(in Chinese with English abstract).
- Yang Y, Luo T Y, Huang Z L, Yang Z S, Tian S H and Qian Z K. 2010b. Sulfur and lead isotope compositions of the Narusongduo silver zinc-lead deposit in Tibet: Implications for the sources of plutons and metal in the deposit[J]. Acta Mineralogical Sinica, 30(3): 311-318(in Chinese with English abstract).
- Yang Z M, Hou Z Q, Xia D X, Song Y C and Li Z. 2008a. Relationship between Western Porphyry and mineralization in Qulong copper deposit of Tibet and its enlightenment to further exploration[J]. Mineral Deposits, 27(1):28-36(in Chinese with English abstract).
- Yang Z M, Hou Z Q, Yang Z S, Wang S X, Wang G R, Tian S H, Wen D Y, Wang Z L and Liu Y C. 2008b. Genesis of porphyries and tectonic controls on the Narigongma porphyry Mo(-Cu) deposit, southern Qinghai[J]. Acta Petrologica Sinica, 24(3): 489-502(in Chinese with English abstract).
- Yang Z M, Hou Z Q, Jiang Y F, Zhang H R and Song Y C. 2011. Sr-Nd-Pb and zircon Hf isotopic constraints on petrogenesis of the Late Jurassic granitic porphyry at Qulong, Tibet[J]. Acta Petrologica Sinica, 27(7): 2003-2010(in Chinese with English abstract).
- Yin A and Harrison T M. 2000. Geologic evolution of the Himalayan-Tibetan orogeny[J]. Annual Review of Earth and Planetary Sciences, 28: 211-280.
- Zang W S, Meng X J, Yang Z S and Ye P S. 2007. Sulfur and lead isotopic compositions of lead-zinc-silver deposits in the Gangdese metallogenetic belt, Tibet, China, and its geological significance[J]. Geological Bulletin of China, 26(10): 1393-1397(in Chinese with English abstract).
- Zhang H F, Xu C W, Guo J Q, Zong K Q, Cai H M and Yuan H L. 2007. Zircon U-Pb and Hf isotopic composition of deformed granite in the southern margin of the Gangdese belt, Tibet: Evidence for Early Jurassic subduction of Neo-Tethyan oceanic slab[J]. Acta Petrologica Sinica, 23(6): 1347-1353(in Chinese with English abstract).
- Zhang Z M, Zhao G C, Santosh M, Wang J L, Dong X and Shen K. 2010. Late Cretaceous charnockite with adakitic affinities from the Gangdese batholith, southeastern Tibet: Evidence for Neo-Tethyan mid-ocean ridge subduction[J]? Gondwana Research, 17(4):615-631.
- Zheng Y C, Fu Q, Hou Z Q, Yang Z S, Huang K X, Wu C D and Sun Q Z. 2015. Metallogeny of the northeastern Gangdese Pb-Zn-Ag-Fe-Mo-W polymetallic belt in the Lhasa terrane, southern Tibet[J]. Ore Geology Reviews, 70: 510-532.
- Zhu D C, Zhao Z D and Niu Y L. 2011. The Lhasa Terrane: Records of a microcontinent and its histories of drift and growth[J]. Earth and Planetary Science Letters, 301: 241-255.

### 附中文参考文献

- 付强,杨竹森,郑远川,黄克贤,段连峰. 2014. 西藏龙马拉Cu-Fe-Pb-Zn多金属矿床金云母Ar-Ar定年及其地球动力学意义[J]. 岩石矿物学杂志, 33(2): 283-293.
- 付强,黄克贤,郑远川,杨竹森,段连峰. 2015. 西藏蒙亚啊铅锌矿床矽卡岩型矿体白云母Ar-Ar年代学研究及其地球动力学意义[J]. 地质学报, 89(3): 569-582.
- 高一鸣,陈毓川,唐菊兴,杜欣,李新法,高明,蔡志超. 2009. 西藏工布江达县亚贵拉铅锌钼多金属矿床石英斑岩锆石SHRIMP定年及其地质意义[J]. 地质学报, 83(10): 1437-1444.
- 高一鸣,陈毓川,唐菊兴,李超,李新法,高明,蔡志超. 2011a. 西藏工布江达地区亚贵拉铅锌钼矿床辉钼矿Re-Os测年及其地质意义[J]. 地质通报, 30(7): 1027-1036.
- 高一鸣,陈毓川,王成辉,侯可军. 2011b. 亚贵拉-沙让-洞中拉矿集区中新生代岩浆岩Hf同位素特征与岩浆源区示踪[J]. 矿床地质, 30(2): 279-291.
- 龚雪婧,杨竹森,赵晓燕,张雄,官玮琦. 2018. 西藏纳如松多铅锌矿区晚白垩世侵入岩形成机制及其地质意义:岩浆锆石证据[J]. 矿床地质, 37(1):91-104.
- 侯增谦,高永丰,孟祥金,曲晓明,黄卫. 2004. 西藏冈底斯中新世斑岩铜矿带: 埃达克质斑岩成因与构造控制[J]. 岩石学报, 20: 239-248.
- 侯增谦,杨竹森,徐文艺,莫宣学,丁林,高永丰,董方浏,李光明,曲晓明,赵志丹,江思宏,孟祥金,李振清,秦克章,杨志明. 2006a. 青藏高原碰撞造山带: I. 主碰撞造山成矿作用[J]. 矿床地质, 25(4): 337-357.
- 侯增谦,莫宣学,高永丰,杨志明,董国臣,丁林. 2006b. 印度大陆与亚洲大陆早期碰撞过程与动力学模型——来自西藏冈底斯新生代火成岩证据[J]. 地质学报, 80(9): 1233-1248.
- 侯增谦,杨志明. 2009. 中国大陆环境斑岩型矿床: 基本地质特征、岩浆热液系统和成矿概念模型[J]. 地质学报, 83(12):1780-1817.
- 侯增谦,郑远川,杨志明,杨竹森. 2012. 大陆碰撞成矿作用: I. 冈底斯新生代斑岩成矿系统[J]. 矿床地质, 31(4): 647-670.
- 黄克贤,郑远川,张松,李为,孙清钟,李秋耘,梁维,付强,侯增谦. 2012. 西藏亚贵拉矿区两期岩体LA-ICP-MS锆石U-Pb定年及地质意义[J]. 岩石矿物学杂志, 31(3): 348-360.
- 纪现华,杨竹森,于玉帅,申俊峰,田世洪,孟祥金,李振清,刘英超. 2012. 西藏纳如松多铅锌矿床成矿岩体形成机制:岩浆锆石证据[J]. 矿床地质, 31(4): 758-774.
- 纪现华,孟祥金,杨竹森,张乾,田世洪,李振清,刘英超,于玉帅.

2014. 西藏纳如松多隐爆角砾岩型铅锌矿床绢云母 Ar-Ar 定年及其地质意义[J]. 地质与勘探, 50(02): 281-290.
- 江万, 莫宣学, 赵崇贺, 郭铁鹰, 张双全. 1999. 青藏高原冈底斯带中段花岗岩类及其中铁镁质微粒包体地球化学特征[J]. 岩石学报, 15(1): 89-97.
- 李献华, 李武显, 王选策, 李秋立, 刘宇, 唐国强. 2009. 幅源岩浆在南岭燕山早期花岗岩形成中的作用: 锆石原位 Hf-O 同位素制约[J]. 中国科学(D辑), 39(7): 872-887.
- 李晓雄, 江万, 梁锦海, 赵志丹, 刘栋, 莫宣学. 2015. 西藏林周盆地发育组玄武岩地球化学特征及意义[J]. 岩石学报, 31(5): 1285-1297.
- 刘英超, 纪现华, 侯增谦, 田世洪, 李振清, 赵晓燕, 周金胜, 马旺, 杨竹森. 2015. 一个与岩浆作用有关的独立铅锌成矿系统的建立——以西藏纳如松多铅锌矿床为例[J]. 岩石矿物学杂志, 34(4): 539-556.
- 刘振声, 王洁民. 1994. 青藏高原南部花岗岩地质地球化学[M]. 成都: 四川科学技术出版社. 1-133.
- 孟祥金, 侯增谦, 叶培盛, 杨竹森, 李振清, 高永丰. 2007. 西藏冈底斯银多金属矿化带的基本特征与成矿远景分析[J]. 矿床地质, 26(2): 153-162.
- 莫宣学, 赵志丹, 邓晋福, 董国臣, 周肃, 郭铁鹰, 张双全, 王亮亮. 2003. 印度-亚洲大陆主碰撞过程的火山作用响应[J]. 地学前缘, 10(3): 135-148.
- 莫宣学, 董国臣, 赵志丹, 周肃, 王亮亮, 邱瑞照, 张凤琴. 2005. 西藏冈底斯带花岗岩的时空分布特征及地壳生长演化信息[J]. 高校地质学报, 11(3): 281-290.
- 莫宣学, 潘桂棠. 2006. 从特提斯到青藏高原形成: 构造-岩浆事件的约束[J]. 地学前缘, 13(6): 43-51.
- 濮巍, 高剑峰, 赵葵东, 凌洪飞, 蒋少涌. 2005. 利用 DCTA 和 HIBA 快速有效分离 Rb-Sr、Sm-Nd 的方法[J]. 南京大学学报(自然科学), 41(4): 445-450.
- 唐菊兴, 陈毓川, 王登红, 王成辉, 许远平, 屈文俊, 黄卫, 黄勇. 2009. 西藏工布江达县沙让斑岩铜矿床辉钼矿铼-锇同位素年龄及其地质意义[J]. 地质学报, 83(5): 698-704.
- 涂光炽, 张玉泉, 赵振华, 王中刚. 1981. 西藏南部花岗岩类的特征和演化[J]. 地球化学, 1: 1-7.
- 王保弟, 许继峰, 刘保民, 陈建林, 王立全, 郭琳, 王冬兵, 张万平. 2013. 拉萨地块北部~90 Ma 斑岩型矿床年代学及成矿地质背景[J]. 地质学报, 87(1): 71-80.
- 王立强, 唐菊兴, 陈毓川, 罗茂澄, 冷秋锋, 陈伟, 王焕. 2011. 西藏帮铺铜(铜)矿床含矿而长花岗斑岩 LA-ICP-MS 锆石 U-Pb 定年及地质意义[J]. 矿床地质, 30(2): 349-360.
- 王立强, 罗茂澄, 袁志浩, 陈伟, 冷秋锋, 张学全. 2012. 西藏帮铺铅锌矿床 S、Pb、C、O 同位素组成及成矿物质来源研究[J]. 地球学报, 33(4): 435-443.
- 王立强, 林鑫, 李壮, 张志, 康浩然, 李海峰. 2014. 西藏蒙亚啊铅锌矿区花岗斑岩年代学、地球化学及 Hf 同位素组成特征[J]. 地质学报, 88(12): 2572-2583.
- 吴福元, 李献华, 杨进辉, 郑永飞. 2007. 花岗岩成因研究的若干问题[J]. 岩石学报, 23(6): 1217-1238.
- 杨勇. 2010. 西藏纳如松多银铅锌矿床地球化学特征研究(博士学位论文)[D]. 导师: 黄智龙, 罗泰义. 贵阳: 中国科学院地球化学研究所. 134 页.
- 杨勇, 罗泰义, 杨竹森, 黄智龙, 田世洪, 钱志宽. 2010a. 冈底斯造山带两套不同成矿体系的含矿斑岩对比研究[J]. 矿床地质, 29(2): 195-206.
- 杨勇, 罗泰义, 黄智龙, 杨竹森, 田世洪, 钱志宽. 2010b. 西藏纳如松多银铅矿 S、Pb 同位素组成: 对成矿物质来源的指示[J]. 矿物学报, 30(3): 311-318.
- 杨志明, 侯增谦, 夏代详, 宋玉财, 李政. 2008a. 西藏驱龙铜矿西部斑岩与成矿关系的厘定: 对矿床未来勘探方向的重要启示[J]. 矿床地质, 27(1): 28-36.
- 杨志明, 侯增谦, 杨竹森, 王淑贤, 王贵仁, 田世洪, 温德银, 王召林, 刘英超. 2008b. 青海纳日贡玛斑岩铜(铜)矿床: 岩石成因及构造控制[J]. 岩石学报, 24(3): 489-502.
- 杨志明, 侯增谦, 江迎飞, 张洪瑞, 宋玉财. 2011. 西藏驱龙矿区早侏罗世斑岩的 Sr-Nd-Pb 及锆石 Hf 同位素研究[J]. 岩石学报, 27(7): 2003-2010.
- 藏文栓, 孟祥金, 杨竹森, 叶培胜. 2007. 西藏冈底斯成矿带铅锌银矿床的 S、Pb 同位素组成及其地质意义 [J]. 地质通报, 26(10): 1393-1397.
- 张宏飞, 徐春旺, 郭建秋, 宗克清, 蔡宏明, 袁洪林. 2007. 冈底斯南缘变形花岗岩锆石 U-Pb 年龄和 Hf 同位素组成: 新特提斯洋早侏罗世俯冲作用的证据[J]. 岩石学报, 23: 1347-1353.